Bima Journal of Science and Technology, Vol. 8(3B) Oct, 2024 ISSN: 2536-6041

DOI: 10.56892/bima.v8i3B.843

Synthesis and Characterization of Cellulose Nano – Crystals Derived from Groundnut Shell for Metronidazole Anti-Biotic Removal

A. M. Hammari, A. J. Abubakar*, A. B. Usman, Fatima M. U., Judith S., Jauro B. M.

[1]Department of Biochemistry, Gombe State University, P.M.B. 127, Gombe, Nigeria.

* Corresponding Author: jauroadamuabubakar1086@gmail.com

ABSTRACT

This research was aimed at investigating the removal of metronidazole (MNZ) an anti-biotic from pharmaceutical wastewater simulated in the laboratory by Cellulose Nano-crystals derived from groundnut shell (CNC-GS). The influence of different factors on the adsorption rate including initial pH, adsorbent dosage, initial MNZ concentration, temperature, and contact time was evaluated. CNCs derived from Groundnut shell was shown to have percentage yield of 33.4%. Fourier transforms infrared spectroscopy, Brunauer–Emmett–Teller technique, X-ray diffraction, and Scanning Electron Microscopy characterized the CNC-GS. The results showed that under the optimal conditions (pH=3, 60 minutes of contact time, an initial MNZ concentration=250 mg/L and a CNC-GS dose of 1.5 g/L), the maximum adsorption efficiency reached 95%. Additionally, kinetic analysis revealed that the pseudo-second-order kinetic model was the most suitable, while the adsorption isotherm closely followed the Langmuir model with R^2 (0.9998). The total pore volume and a micro pore volume of CNC-GS were 0.195 cm^2 /g and 0.139 cm^3 /g, respectively. The total surface area of the adsorbent (CNC-GS) was found to be 380.095m^2 /g. Thermodynamic studies have shown that the reaction was spontaneous (**ΔS** =0.0016628) and endothermic (**ΔH**=0.21283) in nature. In conclusion, CNC-GS proved to be a highly effective adsorbent with a strong capability to remove MNZ from the contaminated water.

Keywords: Metronidazole (MNZ), Cellulose Nano-crystals (CNC-GS), Adsorption efficiency, Kinetic model, Langmuir isotherm.

INTRODUCTION

Antibiotics are a group of chemical compounds that can either kill or inhibit the growth of different bacteria. They are widely used in the prevention and treatment of infections caused by microorganisms (Antonio Marzo, 1998) . The rise of antibiotic-resistant genes (ARGs) is a major global concern, as they are now recognized as environmental contaminants. The potential health risks through dietary exposure cannot be overlooked, as ARGs can infiltrate the food chain and pose direct threats to human health (Patrycja Krasucka, 2021). The increasing use of antibiotics is significantly contributing to environmental pollutions. A large portion, between 30% and 90%, of these drugs is excreted by organisms without being metabolized (Gros *et al.,* 2010). This leads to their persistence in aquatic ecosystems through various channels, including surface runoff, sewage discharges, and waste from livestock.

The overuse of antibiotics in agriculture, aquaculture, and healthcare allows them to enter water bodies without complete removal, jeopardizing ecological balance and human health. The presence of antibiotics can harm the microbiomes of humans and other organisms, disrupting the fragile microbial balance of ecosystems. This disruption may reduce their ability to combat infections and contribute to the rise of antibiotic-resistant bacteria (ARB). Consequently, finding

DOI: 10.56892/bima.v8i3B.843

effective methods to eliminate antibiotic residues is considered a significant global challenge (Mohammadian *et al*., 2024).

Metronidazole (MNZ), as a class of antibiotic, is widely manufactured to treat infections in both humans and animals in many countries. Consequently, huge amount of MNZ antibiotics are often detected in domestic water and food. As a result of their mutagenic and carcinogenic potential, the European Union (EU) has banned the use of Nitroimidazole antibiotics such as MNZ in livestock used for food production (Mohammadian *et al*., 2024). MNZ is a member of Nitroimidazole families, which are target to inhibit and care bacterial infections in both humans and animals. Nevertheless, MNZs are recognized for their poor biodegradability and high toxicity, stemming from their complex molecular structure (Pourzamani *et al.,* 2018). A closed bottle test was conducted to assess the biodegradability of 18 medically significant antibiotics. The results showed that MNZ exhibited only a 1% degradation rate after 54 days at a concentration of 5.95 mg/L (Wen *et al.,* 2019). Another study explored the occurrence and behavior of MNZ in sewage during wastewater treatment, revealing that MNZ was found in 62% of both influent and effluent samples (Mohammadian *et al*., 2024).

Various methods, including biological treatment, membrane filtration, electrochemical techniques, disinfection, immobilization, ion exchange, photocatalysis, and adsorption, have been studied to remove antibiotics from sewage. However, conventional biological treatment systems show limited efficiency in removing antibiotics (Mohammadian *et al*., 2024). Additionally, Sanchez-polo et al., investigated MNZ degradation using gamma irradiation, finding that the toxicity of the by-products exceeded that of the original MNZ. This highlights the urgent need to remove MNZ from water using appropriate technology (Pourzamani *et al.,* 2018). Among these techniques, adsorption stands out for its cost-effectiveness, high efficiency, reusability, and ease of operation. This versatile method allows for the creation of high-quality treated effluents. Furthermore, in cases where adsorption can be reversed adsorbents can be reused after desorption. This flexible approach has significant potential for both environmental and industrial applications (Mohammadian *et al*., 2024).

Carbohydrate polymers, including cellulose and its derivatives, are the most abundant natural materials and can be utilized as adsorbents for water treatment (Nasiri *et al.,* 2022). A huge amount of cheap adsorbents from agro materials such as cucumber peels, meranti sawdust, durian leaf powder, watermelon seed hulls, grape pulp, chitosan, kenaf core fibers, hazelnut Shell, Delonixregia plant leaf have been applied to remove heavy metals and organic solvents from polluted water (Ali *et al.,* 2017). This study focused on examining the adsorption of metronidazole (MNZ) onto Cellulose Nano Crystals (CNCs) derived from Groundnut shell. The effect of adsorbent-adsorbate interactions on adsorption capacity was thoroughly explored. Additionally, the adsorption parameters such as kinetics, thermodynamics and adsorption isotherms were investigated to understand the adsorption mechanism.

MATERIALS AND METHODS

Preparation of Groundnut Shell

Fresh Groundnut shells were collected from Groundnut cultivated area of Kwami local government, Gombe state. The Groundnut shells were washed three times and grinded in a clean mortar and pestle, and shade dried.

DOI: 10.56892/bima.v8i3B.843

Extraction of α-Cellulose

The method reported by Frank *et al.,* (2020) was applied with little modifications. Briefly a 500g of the size reduced groundnut shells above was weighed using electronic balance and transferred into a stainless steel container. A 2% w/v of sodium hydroxide solution prepared was measured and added to the 500 g of the sample above in the container and stirred well to wet the sample. This was transferred to a hot water bath set at 80 °C and left for 4 hours to achieve delignification. The resulting mixture was filtered using a cloth sieve and washed vigorously with excess water and filtered again. The arc was placed in a container, treated with 1:1 dilution of sodium hypochlorite solution (for bleaching) at 95 °C for 30mins on a water bath.

The resulting material was filtered and washed vigorously using sieve cloth and sufficient water. And it was placed back into the stainless steel container and 17.5%w/v of NaOH solution (2.0 L) was added while stirring. Then it was transferred on a water bath set at 80 °C for 1 hour to obtain α-cellulose. The resulting material was also washed with water, filtered and bleached with 1:1 dilution of sodium hypochlorite (700 mL) in a water bath set at 80 °C for a maximum of 15 minutes. It was further filtered with sieve cloth, washed with sufficient water up to five times until tested neutral to litmus paper and then pressed into a big lump followed by a reduction into small lumps, then subsequently dried at 60 °C for 60 minutes in a hot air oven. It was then labeled as Groundnut shell **α-**cellulose and kept for further procedures.

Preparation of Cellulose Nano crystals (Hydrolysis of α-Cellulose)

The method reported by Frank *et al.,* (2020) was used with little alterations. Briefly the α-cellulose obtained above (37g) was weighed and treated with 2.5N hydrochloric acid solution at boiling temperature for 40 minutes in a large glass beaker. The hot acid mixture was then poured into excess tap water in a bucket and stirred vigorously. This was allowed to stand for 18h, the resulting material which sediment at the bottom was filtered with sieve cloth, washed vigorously (until tested neutral to litmus paper) and processed into small lumps which were desiccated in a hot air oven at 60 °C for 60 minutes. The percent yield was calculated and labeled as groundnut shell Cellulose Nano crystals (GH-CNC). This was placed in a desiccator. The GS-CNC obtained was sized reduced using porcelain mortar and pestle, and a fractions were passed through sieve no. 60. The percentage yield was calculated, particulate characteristics of the prepared crystalline cellulose were determined.

Characterization of the synthesized sample

Scanning Electron Microscopy (SEM)

To examine potential changes in the physical structure of the samples, scanning electron microscopy (SEM) analysis was performed. The sample was placed on a double-sided adhesive attached to a sample stub and then coated with a 5 nm layer of gold. It was subsequently inserted into the SEM chamber, where initial focusing and adjustments were done using NaVCaM before switching to SEM mode. Once in SEM mode, the image was fine-tuned for focus and brightness contrast was automatically set. The sample's morphology at different magnifications was then captured and saved to a USB drive.

DOI: 10.56892/bima.v8i3B.843

X-Ray Powder Diffractometer (XRD) Studies

The diffraction patterns and crystallinity of the cellulose materials were analyzed using an X-ray diffractometer. Cu-Kα radiation at 40 kV and 25 mA was used to capture the diffractograms. The powder samples were compressed into pellets with a diameter of 2.50 cm under a pressure of 50 MPa. The crystallinity index (CrI) was calculated according to the equation provided by Frank et al. (2020),

$$CrI = [(I_{002} - I_{am})] / I_{002} \quad (1)$$

Where I_{002} represents the intensity peak around $2\theta = 22°$ and Iam corresponds to the intensity peak near $2\theta = 16°$.

Fourier Transform Infrared (FTIR) Spectroscopy

The study of functional groups and chemical structure of the material prepared from groundnut shell was done using Fourier transform infrared (FTIR) spectroscopic machine (Agilent technology Cary 630 FTIR and Thermo-fisher scientific). Few milligrams of the sample were mixed with KBr, compressed into pellet following standard operating procedures, and this was then scanned at range 4000 to 500 cm^1.

Adsorption Test

Preparation of Standard Solutions

Analytical grade Metronidazole was collected from Pharmaceutics laboratory, Gombe State University. A stock solution of initial drug concentration 1000 mg/l was prepared by dissolving 1 g of powdered drug in 1 L of distilled water. Using molar concentration formula;

$$C_1V_1 = C_2V_2 \quad (1)$$

The actual concentration of the dilute solution was determined using UV-visible Spectrophotometer.

Batch Adsorption Experiment

Adsorption tests were carried out using a metronidazole stock solution (500 mg L^1). Dilution of the stock to 50, 100, 150, 200, 250 mg L^1 was done to carry out the adsorption tests.

Effect of Adsorbents Dosage

Various amounts of GS-CNC (0.5, 1.0, 1.5, 2.0 and 2.5 g) were added to the flask containing 100 mL of MNZ solution (50 mg L^1) at constant pH and room temperature. The samples were shocked gently at 200rpm for 60 minutes and the adsorbent was filtered out of the MNZ solution using a filter paper. UV-Vis spectrophotometer was used to find the MNZ concentration in the spectrophotometric mode.

Effect of pH

GS-CNC (1.5 g) was mixed with 100 mL of MNZ (50 mg L^1) solution with initial pH values of 3, 5, 7, 9 and 10. Sodium Hydroxide NaOH (0.1M) and Hydro Chloric acid HCl (0.1M) were used to adjust the pH of the MNZ solution to the desired pH value and was confirmed by pH meter.

Effect of Contact Time

To evaluate the effects of contact time, 1.5 g of adsorbent was poured into 100 mL each of 50 mg L^1 of MNZ solutions and shaken for 60 minutes at room temperature. The mixtures were removed from the solution at 30, 60, 90, 120 and 150 minutes intervals and were analyzed with UV-Vis spectrophotometer.

Effect of Initial Concentration and Temperature

To determine the effect of temperature and initial concentration, batch adsorption experiment of MNZ onto the adsorbent was carried out in a 250mL airtight Erlenmeyer flask containing 100ml of known concentration of the MNZ solution and precisely measured quantity of the optimum adsorbent dosage (Polycarp, 2018). The

DOI: 10.56892/bima.v8i3B.843

mixture in the flask was agitated on an orbital shaker working at a constant revolution of 200 rpm. The effect of initial MNZ concentration (50, 100, 150, 200, and 250 mg/L, and temperature (298, 303, 313, 323 & 333 K) was computed. The samples in the flask were collected from the shaker at a specified time interval (60 minutes), filtered and the final concentration of the MNZ in the supernatant solutions was investigated using the UV-visible spectrophotometer (Polycarp, 2018).

Equilibrium Adsorption Experiment

Equilibrium adsorption experiments were conducted at a constant room temperature. A measured amount of MNZ solution was added to 250 ml stoppered Erlenmeyer flasks containing a fixed amount of groundnut shell powder and shaken on a mechanical shaker at 200 rpm. Residual MNZ samples were collected from the flasks in batches and filtered. The absorbance of the remaining MNZ was measured at its maximum wavelength of 350 nm using a UV/visible spectrophotometer.

RESULTS AND DISCUSSION

Percentage Yield of Nano Cellulose

Acid hydrolysis using HCl depolymerized α-cellulose to cellulose Nano crystals. The depolymerisation with hydrochloric acid at the fixed 2.5 N concentrations, give percentage yield 33.4% of Nano cellulose. It is observed that the HCl had moderate yield. This might be attributed to its low power to depolymerize α-cellulose.

Characterization Results

FTIR Characterization of CNC - GS Sample

Figure 1 represented the result of FTIR measurement taken for the CNC - GS sample over the frequency range of 4000 to 500cm^{-1}. Absorption band at wavenumber of 3413.15 cm for CNC - GS is attributed to the hydrogen bonded O–H interaction with the surface of the adsorbent (Ahmed *et al.,* 2021). CNC-GS showed the presence of medium peaks at 2925.15 and 2853.78 cm which correspond to the aliphatic C–H stretching (Intidhar *et al*. 2017). Peaks at 1742.74 cm and 1639.55 cm are associated with C=O stretch of esters and C=C of alkenes respectively. Also displayed is the C-H bending at 1458.23 cm. The peaks at 1124.54 cm and 1033.88 cm demonstrated the aliphatic amine C-N stretching. Meanwhile, peak at 1157.33 cm corresponds to the alkyl halide C-H wagging.

SEM Characterization of CNC - GS materials

The surface morphology of the adsorbent was evaluated using SEM micrographs. The SEM micrograph of the CNC-GS (Plate I (a) (b) and (c)) at different magnifications range of 2000x, 1000x and 500x shows a form of rough surface with visible pores that are suitable for adsorption.

BET Characterization

BET result of the CNC-GS material which is characteristic of its surface textural analysis and include its multi-point BET specific surface area, BJH total pore volume, BJH average pore width and HK micro pore volume are presented in table 1. The CNC - GS showed very large BET surface area and moderate total pore volume.

XRD Characterization

Figure 2 shows the XRD patterns of CNC-GS. A number of characterization peaks for CNC-GS (2θ = 13°, 10°, 35°, 15° , 33°, and 18°, corresponding to their indices 23, 17, 12, 6, 18, and 24, respectively) were detected. The data conform to the information of previous research work (Pourjavadi *et al*., 2015).

Bima Journal of Science and Technology, Vol. 8(3B) Oct, 2024 ISSN: 2536-6041

DOI: 10.56892/bima.v8i3B.843

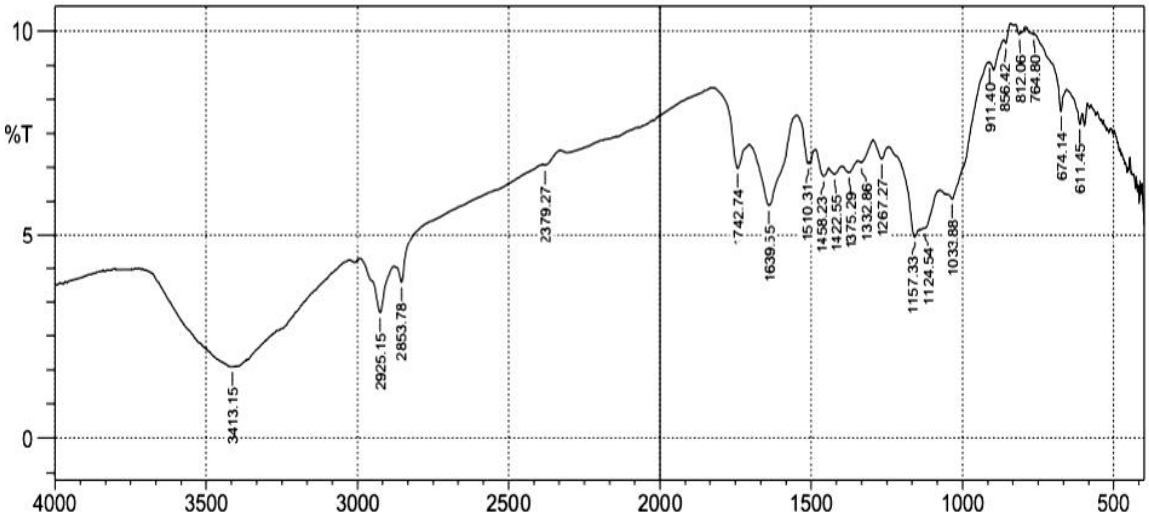

Figure 1: Shows the result of FTIR analysis of CNC-GS.

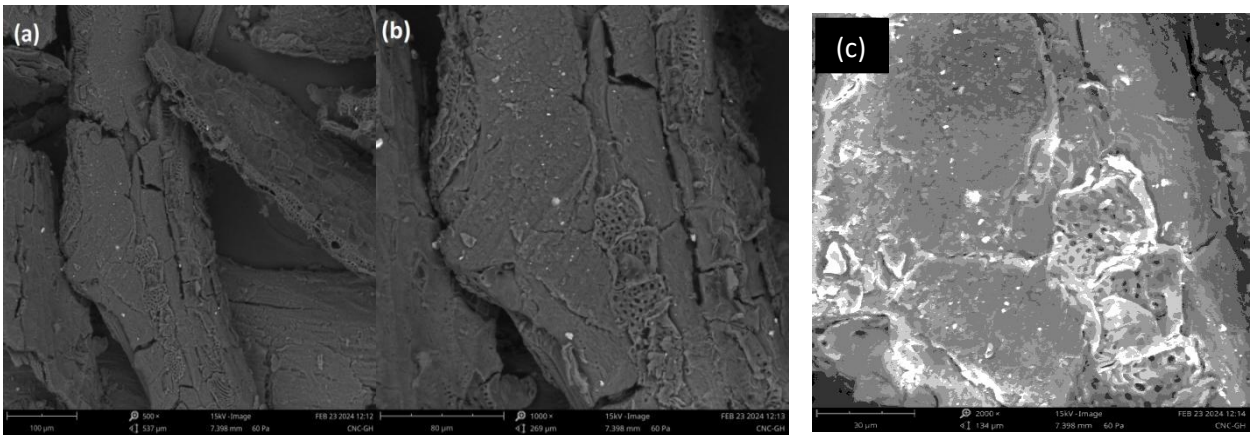

Plate I; (a) 500x (b) 1000x (c) 2000x: SEM Image of CNC - GS Material

Table 1: BET Result of CNC - GS material

BET Surface area (m^2/g)	Total pore volume (cm^3/g)	Micro pore volume (cm^3/g)	Average pore width (nm)	Mesoporosity (%)
380.095	0.195	0.139	2.153	71%

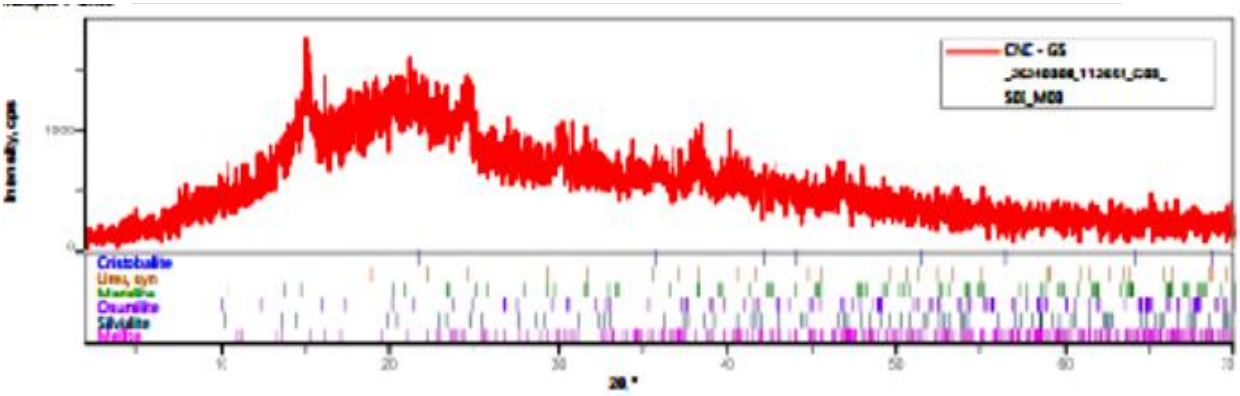

Figure 2: XRD patterns of CNC-GS.

DOI: 10.56892/bima.v8i3B.843

Batch Adsorption Study

To determine the adsorption characteristics of CNC-GS, adsorption tests were performed using laboratory base simulated MNZ solution. The details of the experiment are demonstrated in the subsequent sections.

The Effects of Initial Concentration on Adsorption

The effect of the initial MNZ concentration on CNC-GS showed that maximum adsorption occurred as the concentration increased from 50 mg/L to 250 mg/L. For example, the MNZ removal efficiency at concentrations of 50 mg/L, 100 mg/L, 150 mg/L, 200 mg/L, and 250 mg/L was 93.77%, 95.54%, 97.80%, 98.08%, and 99.00%, respectively. This high percentage of removal can be attributed to mass transfer phenomena (diffusion) caused by the concentration gradient between the adsorbent and adsorbate. At a low MNZ concentration of 50 mg/L, for instance, the active adsorption sites of the adsorbent are quickly occupied and saturated by sorbate molecules, leading to lower removal efficiency. However, at a higher initial concentration of 200 mg/L, a greater adsorbent-adsorbate ratio was achieved due to the increased number of adsorbate molecules, resulting in higher adsorption efficiency. Thus, a higher initial concentration enhances the MNZ adsorption process (Patil et al., 2011). This increased removal efficiency may be due to the adsorbent's BET specific surface area and/or ionic interactions between the adsorbent and adsorbate (Patil et al., 2011).

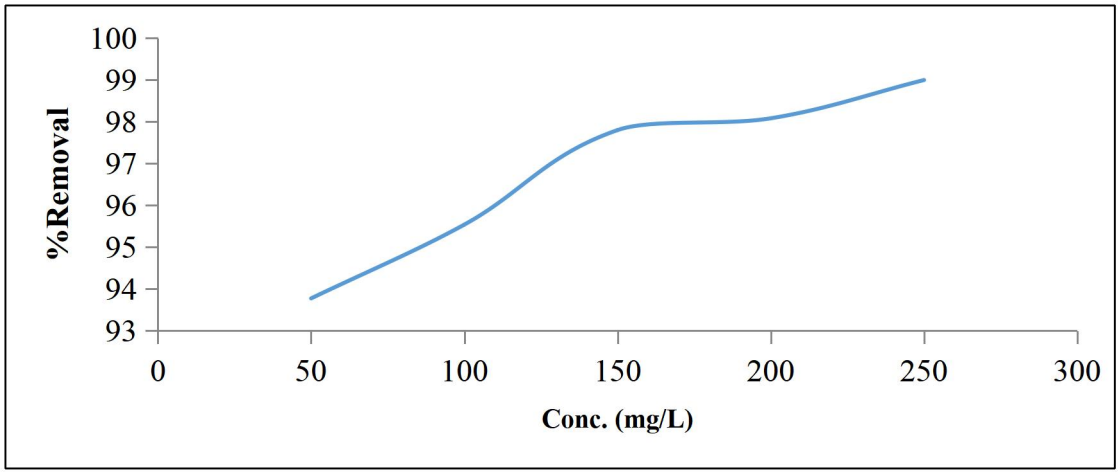

Figure 3: Effect of initial concentration of metronidazole on adsorption.

The Effect of Adsorbents Dosage on Metronidazole Adsorption

Figure 4 shows the percentage adsorbed of MNZ on CNC - GS at various adsorbent dosages. It is clear from the Figure 4 that the CNC-GS adsorbed most of the MNZ even at the lowest dose of 0.5g. Hence, the adsorption capacity of CNC-GS upsurges with the increase in adsorbent dose.

However, the optimum equilibrium was reached at dose 1.5g. Thus, no noticeable increased in removal efficiency of MNZ beyond that dosage (figure 4). Therefore 1.5g is considered as optimum equilibrium and was used in the subsequent steps. The optimum adsorption of MNZ on CNC-GS at very small quantity of adsorbent dosage is attributed to the large surface and porosity of CNC-GS (Hammari et al., 2020). The increased in removal efficiency with increased in adsorbent dosage is probably as a result of presence of more surface area and pores, because of the

DOI: 10.56892/bima.v8i3B.843

availability of more adsorbent (Hammari *et al.,* 2020).

Although the percentage removal efficiency increased as the adsorption sites on the adsorbent surface became occupied, the adsorption capacity decreased (Hoseinzadeh et al., 2018; Khosravi et al., 2018). The findings of this study align with those reported by Khosravi et al., 2018 who used modified montmorillonite with ZnO and TiO2 nanoparticles, along with H_2O_2, to remove cephalexin from aqueous solutions. They found that the percentage of cephalexin removal, initially 33%, increased as the amount of green local montmorillonite (GLM) was raised from 0.4 to 4 g/L (Khosravi et al., 2018).

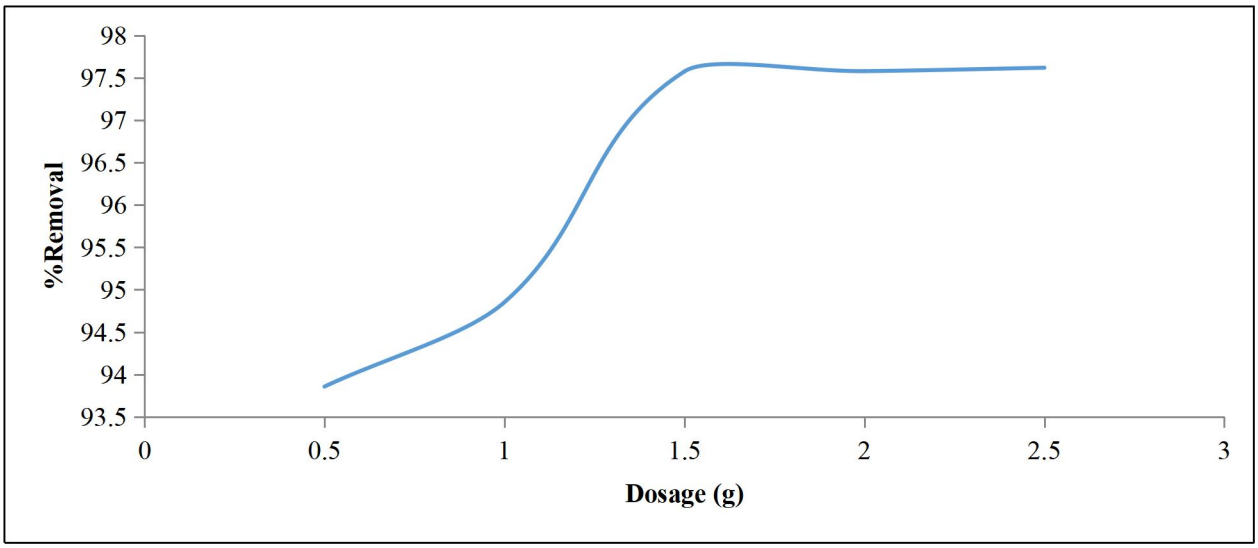

Figure 4: Effect of adsorbent dosage on metronidazole adsorption.

The Effect of Contact Time on Metronidazole adsorption

Data of the effect of contact time (30, 60, 90,120 and 150 min) on MNZ adsorption upon CNC-GS are presented in Figure 5. The adsorption of the MNZ occurred during the first 60 minutes where, at 120 minutes the equilibrium was attained. This showed that the process is very rapid. The rapidly adsorption can be attributed to the presence of more free adsorption sites at the beginning of the adsorption process where the MNZ was being adsorbed (Hammari et al., 2020).

Adsorption abruptly stopped after all of the available sites were occupied, hence, equilibrium was reached. The process was prolonged to 150 minutes to obtain complete equilibrium, even though; the equilibrium was attained within first 120 minutes. Information from the previous researches demonstrated a similar mechanism of the adsorbents (Hammari et al., 2020). Adsorbent materials differed in their specific optimum equilibrium time. Most of the previous studies demonstrated equilibrium time of 90–150 minutes. The nature of the surface area and pore volumes of the adsorbents influenced equilibrium time.

DOI: 10.56892/bima.v8i3B.843

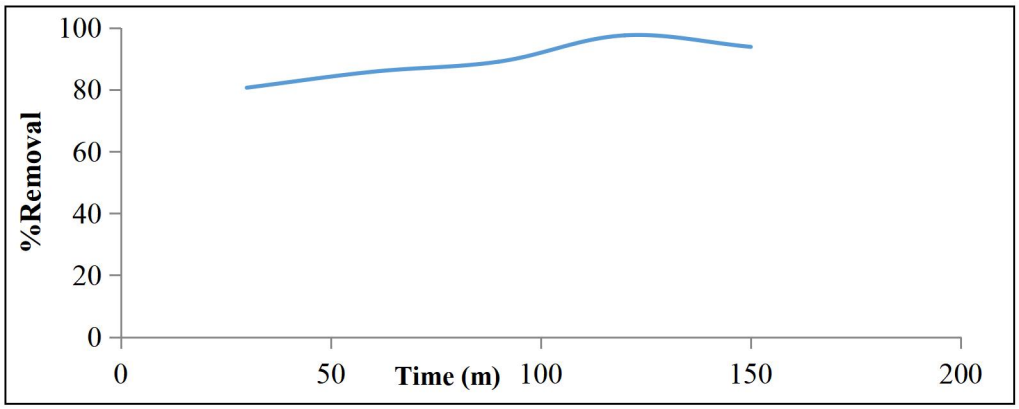

Figure 5: Effect of Contact Time on Metronidazole adsorption.

The Effect of pH on Metronidazole adsorption

The adsorption capacity decreased as the pH increased. For example, the amount of MNZ adsorbed at pH 3 and pH 11 was 97.61% and 80.63%, respectively. Therefore, pH 3 was considered the optimal pH and was used for the remainder of the experiment. This can be explained by the point of zero charge (pHzc), the pH at which surface charges become neutral. Typically, the pH of the adsorbent significantly affects the adsorption process; at pH levels below the pHzc, a positive charge develops on the surface. The high percentage of MNZ removal in acidic conditions (low pH) suggests that the MNZ was adsorbed onto GS-CNC via its carboxyl groups (Mousel et al., 2021).

At higher pH levels, the adsorption capacity decreased due to reduced electrostatic attraction between MNZ and the negatively charged sites on the GS-CNC surface. The effectiveness of MNZ removal declined as the number of hydroxyl groups increased with rising pH, which typically reduces the number of positively charged adsorption sites (Mousel et al., 2021).

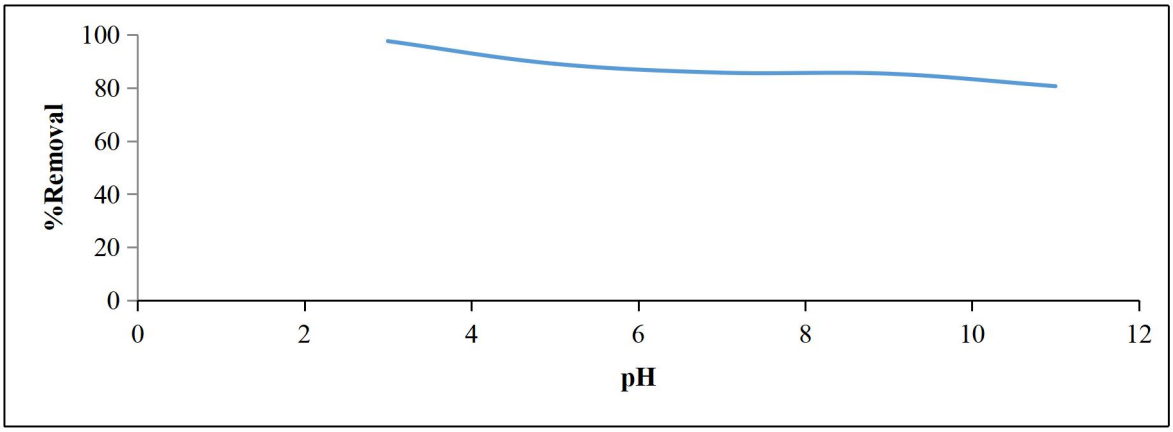

Figure 6: Effect of pH on Metronidazole adsorption.

The Effect of Temperature on Metronidazole Adsorption

The result stated that as the adsorption temperature rose from 25 to 50℃, there was increased in the percentage removal capacity from 88.42% to 94.469% on the CNC-GS (figure 7). When adsorption temperature was initially increased from 25℃ to 50℃ for the

DOI: 10.56892/bima.v8i3B.843

adsorbent, adsorbate materials move more rapidly because of decreased viscosity and collided fast with the adsorbent outer boundary layers and inner pores, resulting in increasing the removal efficiency. Meantime, farther rise in the adsorbate temperature beyond 50 ℃ , led to deformation of the adhesive forces that attached the adsorbate and adsorbent which caused the removal efficiency to be reduced (Ahmed *et al.,* 2015).

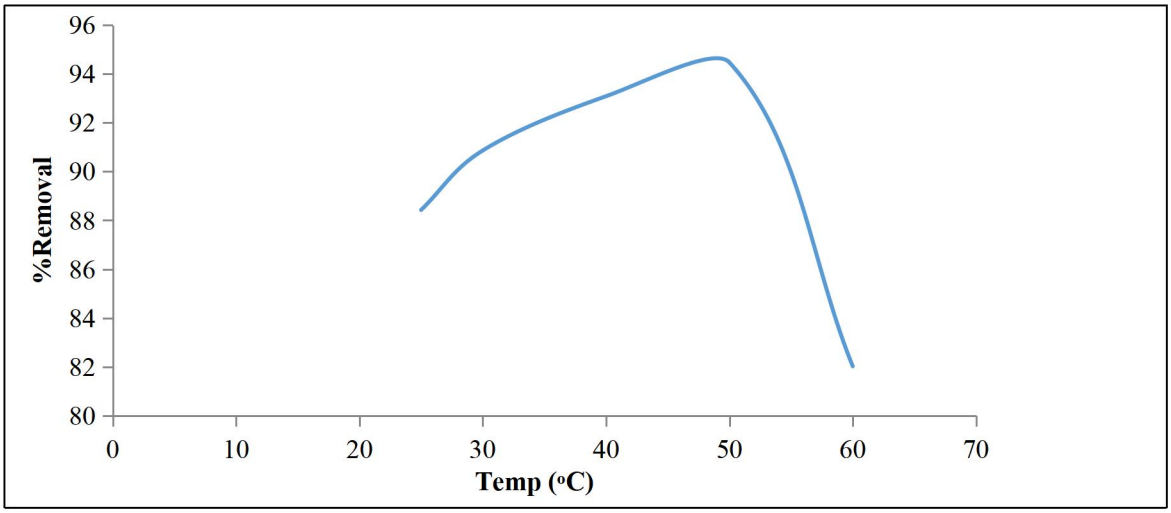

Figure 7: Effect of temperature on Metronidazole adsorption.

Isotherm Models for MNZ Removal

To understand the adsorption mechanism of MNZ on CNC-GS, data from the batch adsorption experiments were plotted using two common models: the Langmuir isotherm model and the Freundlich isotherm model. Figure 8 displays the isotherms derived from these models, while Table 2 lists the correlation coefficients for the adsorption isotherm models. As shown in Table 2, the R^2 value for the CNC-GS adsorbent in the Langmuir isotherm model was higher than that in the Freundlich model, indicating that the adsorption process followed the Langmuir isotherm model more closely. Additionally, the value of KL ranged between 0 and 1, confirming that MNZ adsorption by CNC-GS was favorable. In the Freundlich isotherm model, the value of n was greater than 1, suggesting that the MNZ adsorption process on the adsorbent was physical and favorable (Makeswari et al., 2016).

Table 2: Equilibrium Isotherms Parameters for MNZ Removal.

Models	Parameters	
Langmuir	q_m (mg/g)	0.003
	K_L (1/mg)	0.002
	R^2	0.9998
Freundlich	K	0.7133
	n	9.1825
	R^2	0.9379

Bima Journal of Science and Technology, Vol. 8(3B) Oct, 2024 ISSN: 2536-6041

DOI: 10.56892/bima.v8i3B.843

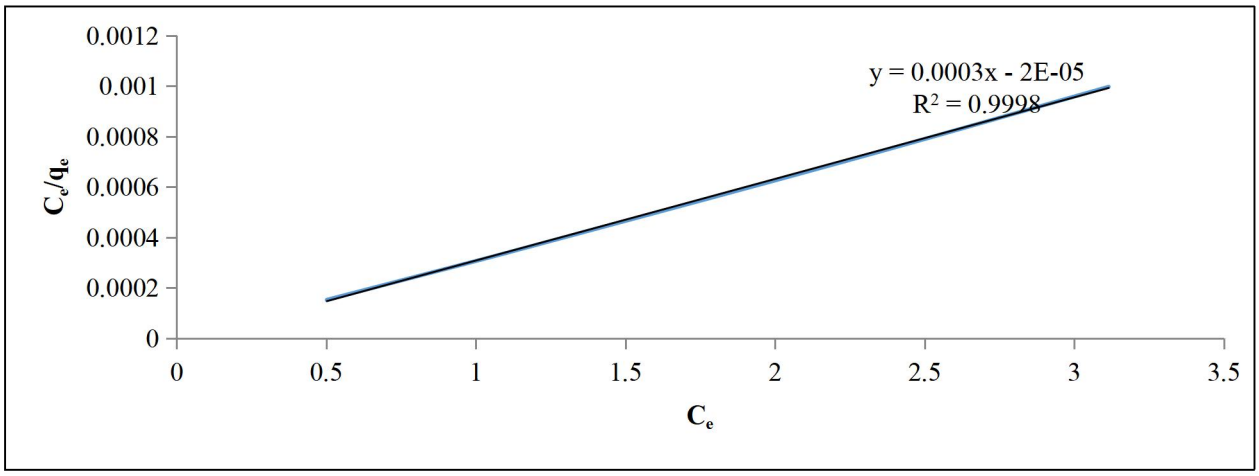

Figure 8: Langmuir Isotherm Model for MNZ removal.

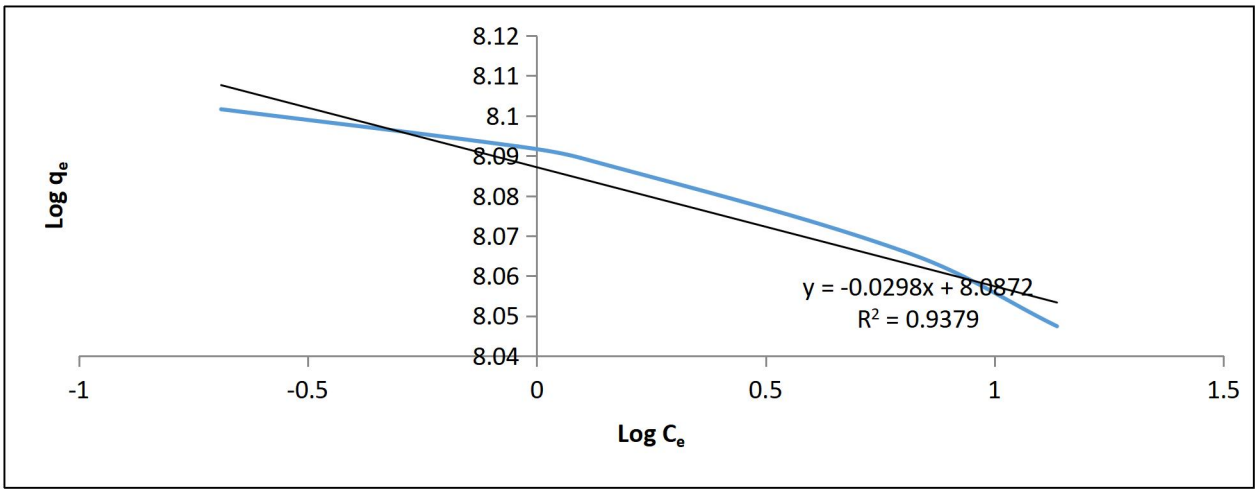

Figure 9: Freundlich Isotherm Model for Metronidazole Removal.

Kinetic Models

To investigate the rate of movement of MNZ mass on the adsorbent CNC-GS, kinetic parameters were evaluated using the set of data obtained from the pseudo-first-order and pseudo-second-order models.

By considering the values of kinetic constants and the regression values R^2epresented in Table 3 and Figure 11, and by also relating the calculated data to the experimental data, it can be pointed out that the rate of the adsorption best fitted the pseudo second-order kinetic model. Research reported by Al-Khalisy *et al*. (2010) observed that removal of cephalexin from aqueous solutions by bentonite and activated carbon best fitted the pseudo-second-order model (Al-Khalisy *et al*. 2010).

Table 3: Kinetic Model Parameters for Metronidazole Removal.

Kinetic Model	Parameters	GS
Pseudo First Order	q_e (mg/g)	6.4814
	K_1 (min^{-1})	0.0014
	R^2	0.8359
Pseudo Second Order	q_e (mg/g)	0.0035
	K_2 (g/ mg min)	0.0004
	R^2	0.9953

Bima Journal of Science and Technology, Vol. 8(3B) Oct, 2024 ISSN: 2536-6041

DOI: 10.56892/bima.v8i3B.843

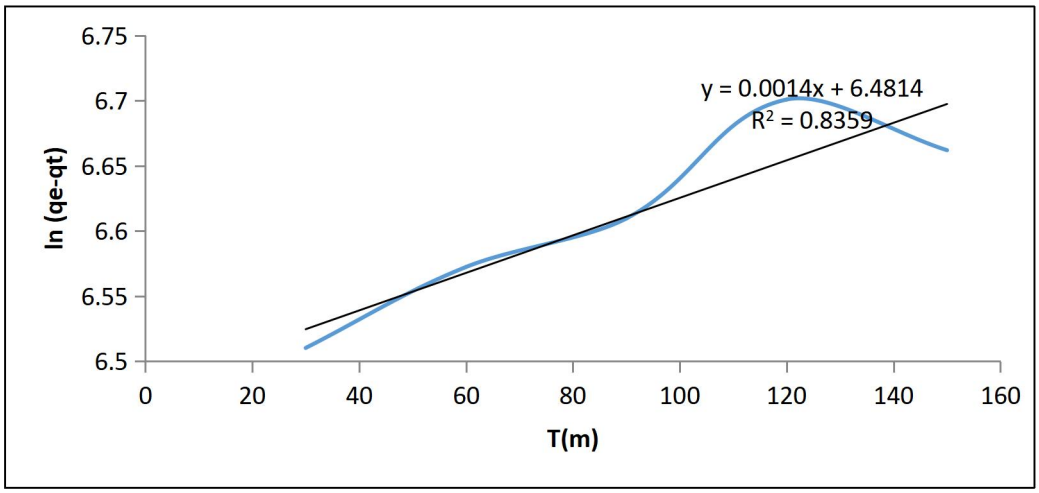

Figure 10: Pseudo First Order Kinetic Model for Metronidazole Removal.

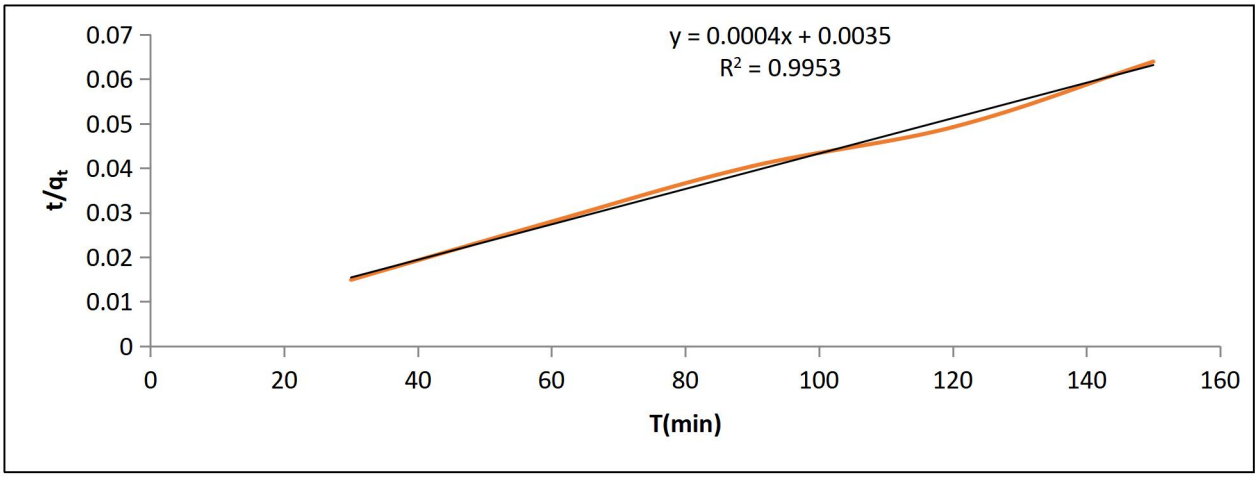

Figure 11: Pseudo Second Order Kinetic Model for Metronidazole Removal.

Thermodynamics Parameters

All thermodynamic parameters for Adsorption of MNZ onto CNC-GS are presented in Table 4. The ΔG values, change from -0.49516 to -0.5536, while the temperature increases from 298 to 333. The negative sign in values for ΔG demonstrated that the process of MNZ adsorption is spontaneous in nature at all the various temperatures for CNC-GS. The values of ΔG reduced with increasing temperature which clearly demonstrated that adsorption of MNZ on CNC-GS is unfavorable (Enenebeaku *et al.,* 2015). The positive sign in values for ΔH demonstrated that the process does not consume energy (endothermic) during adsorption. The positive sign in values for ΔS demonstrated that entropy increased at the solid – solute interface during reaction.

Table 4: Thermodynamic Parameters for Metronidazole Removal.

	Temperature (K)	ΔG (J/mol)	ΔS (J/molK)	ΔH (J/mol)
GS	298	-0.49516		
	303	-0.50347		
	313	-0.5201	0.0016628	0.21283
	323	-0.53673		
	333	-0.5536		

DOI: 10.56892/bima.v8i3B.843

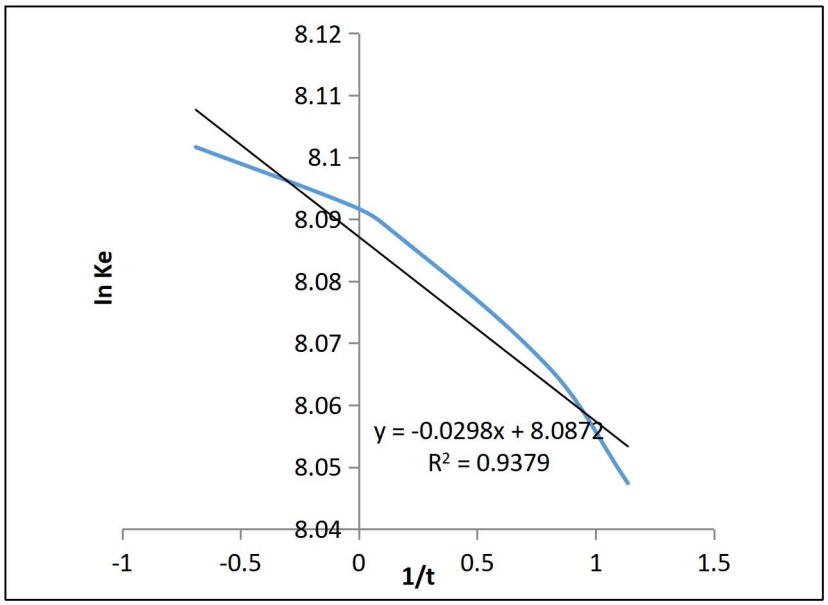

Figure 12: Thermodynamic Plot for Metronidazole Removal.

CONCLUSION

In this research, synthesis and characterization of Cellulose Nano Crystals from an agro waste (Groundnut Shell) was carried out. Adsorption potential of MNZ on the CNC-GS was also determined. The results demonstrated that groundnut shell has percentage yield of 33.4%, and the sorption of MNZ is more favorable in low pH and adsorption capacity reduced with increasing initial concentration. The data from the adsorption kinetic study and adsorption isotherm study indicated that the adsorption of MNZ was directly proportional to the pseudo-second-order and Langmuir models. Thus, it can be deduced that the MNZ adsorption process is physical process. 380.095cm3 and 0.195 cm3 /g are the surface area and the total pore volume of CNC-GS respectively. Additionally, thermodynamic parameters ($\Delta G, \Delta H$ *and* ΔS) showed that the process of the adsorption is spontaneous and does not consume energy (endothermic). The findings of this study demonstrated that Cellulose Nano crystals (CNCs) derived from Groundnut shells is capable of removing metronidazole antibiotics from synthetic wastewater.

REFERENCES

Ahmed Zelekew, Adugna Boke Abdeta, Dong-Hau Kuo, Qinhan Wu, Jubin Zhang, Zhanhui Yuan, Jinguo Lin, Xiaoyun Chen. Biological renewable nanocellulose templated CeO2/TiO2 synthesis and its photocatalytic removal efficiency of pollutants Huizhi Sun a, Yuanbo Guo a, Osman. Journal of Molecular Liquids 336 (2021) 116873

Ahmed, M. B.; Zhou, J. L.; Ngo, H. H.; Guo, W. Adsorptive removal of antibiotics from water and wastewater: Progress and challenges. Sci. Total Environ. 2015, 532, 112−26.

Ali I, AL-Othmanb ZA, Alwarthan A (2016) Synthesis of composite iron nano adsorbent and removal of ibuprofen drug residue from water. J Mol Liq 219:858–864.

Ali Rizakul, N. S. (2017). Kinetics and Thermodynamics Studies of Adsorption of Methylene Blue from Aqueous Solutions onto Paliurusspina-christiMill. Fruits and Seeds. . *IOSR Journal of Applied Chemistry (IOSR-JAC) e-ISSN:*

DOI: 10.56892/bima.v8i3B.843

2278-5736.Volume 10, Issue 5 Ver, I (May, 2017), PP 53-63.

Alireza Nasiri, M. R. (2022). New efficient and recyclabe magnetic nanohybrid adsrbent for the metronidazole removal from simulated wastewater. *Journal of Materials Science: Materials in Electronics*, Volume 33, page 25103-25126.

Antonio Marzo, L. D. (1998). Chromatography as an analytical tool for selected antibiotic classes: a reappraisal addressed to pharmacokinetic application. *Journal of Chromatography A*, Volume 812, Issues 1-2, Pages 17-34.

Enenebeaku K. Conrad, Okorocha J. Nnaemeka and Akalezi O. Chris (2015) "Adsorptive Removal of Methylene Blue from Aqueous Solution Using Agricultural Waste: Equilibrium, Kinetic and Thermodynamic Studies"American Journal of Chemistry and Materials Science 2015; 2(3): 14-25

Frank O Ohwoavworhua, Augustine O Okhamafe (2020) Cellulose nanocrystals and nanofibrils obtained from corn straw by hydrolytic action of four acids: particulate, powder and tablet properties. DRUG DISCOVERY/ANALYSIS VOL.14, ISSUE 34, 2020

Hamidreza Pourzamani, N. M. (2018). Comparison of electrochemical advanced oxidation process for removal of ciprofloxacin from aqueous solutions. *Desalination and Water Treatment*, Volume.

Hammari Abubakar M., Hayatuddeen Abubakar, M. I. Misau, U. O. Aroke and U.D Hamza. Adsorption Equilibrium and Kinetic Studies of Methylene Blue Dye Using Groundnut Shell and Sorghum Husk Biosorbent, Journal of Environmental Bioremediation and Toxicology Website:http://journal.hibiscuspublisher.com/index.php/JEBAT/index. JEBAT, 2020, Vol 3, No 2, 32-39

Hassanzadeh, Masoumeh, "Nanocellulose from the Appalachian Hardwood Forest and Its Potential Applications" (2018). Graduate Theses, Dissertations, and Problem Reports. 5780. https://researchrepository.wvu.edu/etd/5780

Hosseinzadeh, Masoumeh, "Nanocellulose from the Appalachian Hardwood Forest and Its Potential Applications" (2013). Graduate theses Dissertations and Problem Reports. 5780.

Intidhar J Idan, Luqman C Abdullah, Thomas S Y Choong, Siti NurulAin B., M. D. Jamil (2017) Equilibrium, kinetics and thermodynamic adsorption studies of acid dyes on adsorbent developed from kenaf core fiber, Adsorption Science & Technology 1–19

Kamaraj M. and P. Umamaheswari (2017) Preparation and characterization of Groundnut shell activated carbon as an efficient adsorbent for the removal of Methylene blue dye from aqueous solution with microbiostatic activity, Journal of Materials and Environmental Sciences ISSN : 2028-2508 JMES, 2017 Volume 8, Issue 6, Page 2019-2025.

Khosravi panel Rasoul , Hadi Eslami, Ahmad Zarei, Moh sen Heidari, Abbas Norouzian Baghani, Navid Safavi, Adel Mokammel, Mehdi Fazlzadeh, Shahin Ad hami Comparative evaluation of nitrate adsorption from aqueous solutions using green and red local montmorillonite adsorbents. Desalination and Water Treatment Volume 116, June 2018, Pages 119-128

Makeswari M, Santhi T and Ezhilarasi MR (2016) Adsorption of methylene blue dye by citric acid modified leaves of Ricinuscommunis from aqueous solutions.

DOI: 10.56892/bima.v8i3B.843

Journal of Chemical and Pharmaceutical Research 8(7): 452–462.

Meritxell Gros, M. P. (2010). Reomval of Pharmaceuticals during wastewater treatment and environmental risk assessment using hazard indexes. *Environmental International*, Volume 36, 15-26.

Mousel D., D. Bastian, J. Firk, L. Palmowski, J. Pinnekamp, Removal of pharmaceuticals from wastewater of health care facilities, Sci. Total Environ. 751 (2021) 141310.

Negar Mohammadian, T. T. (2024). PW12/Fe3O4/biochar nanocomposite as an efficient adsorbent for metronidazole removal from aqueous solution: Synthesis and Optimization. *Surfaces and Interfaces*, Volume 52.

Patil, S., Renukdas, S. and Patel, N. (2011). Removal of methylene blue, a basic dye from aqueous solutions by adsorption using teak tree (Tectonagradnic) bark powder.*Inter. J. Env. Sci.* 1(5): 711 – 726.

Patrycja Krasucka, B. P. (2021). Engineered biochar- A sustainable solution for the removal of antibiotics from water . *Chemical Engineering Journal*, Volume 405.

Polycarp Datugun (2018) Adsorption Of Dyes On Sorghum Husk And Grounnut Shell From Agricultural Wastes. Theses at AbubakarTafawaBalewa University, Bauchi.

Pourjavadi, A. Z. Mazaheri Tehrani, S. Jokar, Chitosan based supramolecular polypseudorotaxane as a pH-responsive polymer and their hybridization with mesoporous silica-coated magnetic graphene oxide for triggered anticancer drug delivery, Polymer 76 (2015) 52–61.

Xiaofeng Wen, Z. Z. (2019). Immobilised laccase on bentonite-derived mesoporous materials for removal of tetracycline. *Chemosphere*, Volume 222, 865-871.